ACS APPLIED MATERIALS & INTERFACES

Research Article

Cite This: ACS Appl. Mater. Interfaces XXXX, XXX, XXX−XXX

www.acsami.org

Medium-Bandgap Small-Molecule Donors Compatible with Both Fullerene and Nonfullerene Acceptors

Yong Huo,[†] Cenqi Yan,[§] Bin Kan,[∥] Xiao-Fei Liu,[†] Li-Chuan Chen,[†] Chen-Xia Hu,[†] Tsz-Ki Lau,[⊥] Xinhui Lu,[⊥] Chun-Lin Sun,[†] Xiangfeng Shao,[†] Yongsheng Chen,*[,∥] Xiaowei Zhan,*[,§] and Hao-Li Zhang*[,†,‡]

[†]State Key Laboratory of Applied Organic Chemistry, Key Laboratory of Special Function Materials and Structure Design, College of Chemistry and Chemical Engineering, Lanzhou University, Lanzhou 730000, China

[‡]Tianjin Key Laboratory of Molecular Optoelectronic Sciences, Department of Chemistry, Tianjin University, and Collaborative Innovation Center of Chemical Science and Engineering (Tianjin), Tianjin 300072, P. R. China

[§]Department of Materials Science and Engineering, College of Engineering, Key Laboratory of Polymer Chemistry and Physics of Ministry of Education, Peking University, Beijing 100871, China

[∥]Key Laboratory of Functional Polymer Materials and the Centre of Nanoscale Science and Technology, Institute of Polymer Chemistry, College of Chemistry, Nankai University, Tianjin 300071, China

[⊥]Department of Physics, The Chinese University of Hong Kong, New Territories, Hong Kong, China

Supporting Information

ABSTRACT: Much effort has been devoted to the development of new donor materials for small-molecule organic solar cells due to their inherent advantages of well-defined molecular weight, easy purification, and good reproducibility in photovoltaic performance. Herein, we report two small-molecule donors that are compatible with both fullerene and nonfullerene acceptors. Both molecules consist of an (E)-1,2-di(thiophen-2-yl)ethane-substituted (TVT-substituted) benzo[1,2-b:4,5-b′]dithiophene (BDT) as the central unit, and two rhodanine units as the terminal electron-withdrawing groups. The central units are modified with either alkyl side chains (DRBDT-TVT) or alkylthio side chains (DRBDT-STVT). Both molecules exhibit a medium bandgap with complementary absorption and proper energy level offset with typical acceptors like $PC_{71}BM$ and IDIC. The optimized devices show a decent power conversion efficiency (PCE) of 6.87% for small-molecule organic solar cells and 6.63% for nonfullerene all small-molecule organic solar cells. Our results reveal that rationally designed medium-bandgap small-molecule donors can be applied in high-performance small-molecule organic solar cells with different types of acceptors.

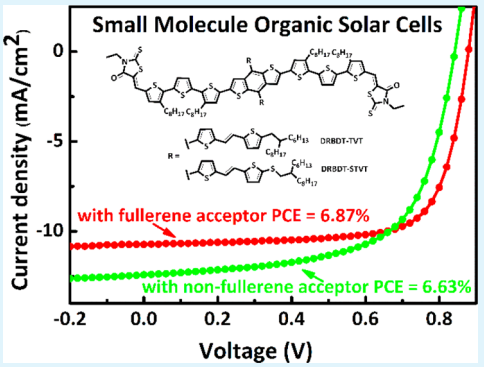

KEYWORDS: *small-molecule donor, fused-ring electron acceptor, compatibility, fullerene organic solar cell, nonfullerene organic solar cell*

INTRODUCTION

Organic solar cells (OSCs) have aroused considerable interest in the past few decades due to their many attractive features, such as solution-processability, light weight, flexibility, and semitransparency.[1−4] OSCs constructed with bulk heterojunction (BHJ) architectures contain donor and acceptor materials.[5,6] Fullerene derivatives have been the predominant acceptor materials for decades. The superiority of the fullerene derivative acceptors includes excellent electron mobility, high electron affinity, and easy formation of an appropriate phase separation with donor materials. The power conversion efficiencies (PCEs) of fullerene-based OSCs have broken 10%.[7−11] However, fullerene derivatives have inherent shortcomings including weak absorption in the visible region and nearly fixed energy levels, which limits the further improvement of photovoltaic performance.[12,13] Recently, nonfullerene organic solar cells (NF-OSCs) have made rapid progress partially due to the fast devolvement of nonfullerene acceptor materials.[14−18] Nonfullerene acceptors based on fused-ring electron acceptors (FREAs), such as ITIC[19] and IDIC,[20] have met much success, due to their enhanced and broadened absorption in the visible-to-near-infrared region, optimal energy levels, and less energy loss in the device.[21−31] The record PCEs of over 13% obtained from NF-OSCs even have surpassed those of fullerene-based solar cells.[32,33]

Electron donor materials often employ electron-rich conjugated polymers or small molecules.[34−45] Early research on donor materials has focused on polymer donors, while

Received: November 24, 2017
Accepted: February 28, 2018
Published: February 28, 2018

DOI: 10.1021/acsami.7b17961
ACS Appl. Mater. Interfaces XXXX, XXX, XXX−XXX

small-molecule (SM) donors have been drawing increasing attention in recent years. Compared with polymers, SM donors have several advantages, including good crystallinity, accurate molecular weight, and well-defined chemical structure. Although the development of SM donors lagged behind the polymer ones in the early stages, PCEs of small-molecule organic solar cells (SM-OSCs) have now reached over 11%, abreast to that of polymer solar cells.[7,46,47] For nonfullerene all small-molecule organic solar cells (NFASM-OSCs), though the best PCE has achieved about 10%,[48−50] most cells can only give PCEs below 6%.[51−54] As SM donors with excellent PCE performance are still limited in either SM-OSCs or NFASM-OSCs, significant efforts are being devoted to the design and synthesis of novel high-performance SM donors for both SM-OSCs and NFASM-OSCs.

In the past two decades, fullerene derivatives have been widely used as model acceptors in organic solar cells, in combination with a broad range of donor materials. In fact, the dominant role of the fullerene acceptor in OSC research has allowed researchers to concentrate their efforts on donor materials and thus dramatically reduced the work load. Unlike the situation in acceptor materials, there are a few types of SM donor that are suitable for different acceptors. In the literature, most reported SM donors either exhibited low PCEs or showed better performance with one type of acceptor over the others.[55,56] Developing a general type of SM donor that can work well with both the fullerene acceptor and small-molecule nonfullerene acceptor is highly desirable under the current situation that more and more new acceptors are emerging. A widely applicable universal SM donor may not give the highest PCE, but could significantly simplify the efforts in material screening and device optimization. Moreover, developing SM donors that can match well with both fullerene and nonfullerene acceptors can also provide new insights to the relationship between material and performance.

However, it is highly challenging to design SM donors compatible with both fullerene and nonfullerene acceptors, as they have different requirements in absorption spectra, energy level, and morphology control.[57] It is considered that a universal SM donor should meet the following criteria. First, it should have a medium optical bandgap to present complementary absorption with the common acceptors. Second, the highest occupied molecular orbital (HOMO) and lowest unoccupied molecular orbital (LUMO) should position appropriately compared with the fullerene or nonfullerene acceptors, to produce enough thermodynamic driving force for charge separation and to reduce the energy loss. Third, an acceptor−donor−acceptor (A−D−A) or similar structure is necessary to enhance intramolecular charge transfer and to achieve high absorption coefficients.

The molecules DRBDT-TVT and DRBDT-STVT (Figure 1) were designed under the above considerations. These molecules consist of benzo[1,2-b:4,5-b′]dithiophene (BDT) moieties substituted by (E)-1,2-di(thiophen-2-yl)ethane (TVT) as the central building block, and the 3-ethylrhodanine as the ending electron-withdrawing group. BDT is a widely applied conjugated moiety for building polymers and SM donors due to its symmetric and planar structure.[58] For instance, Hou and Kang et al. reported that BDT units incorporating TVT side groups could lead to red-shifted and enhanced absorption, thereby boosting the short circuit current (J_{SC}).[59,60] Considering the recent reports that the alkylthio substituent may downshift the HOMO energy level and affect hole mobility,[61−63]

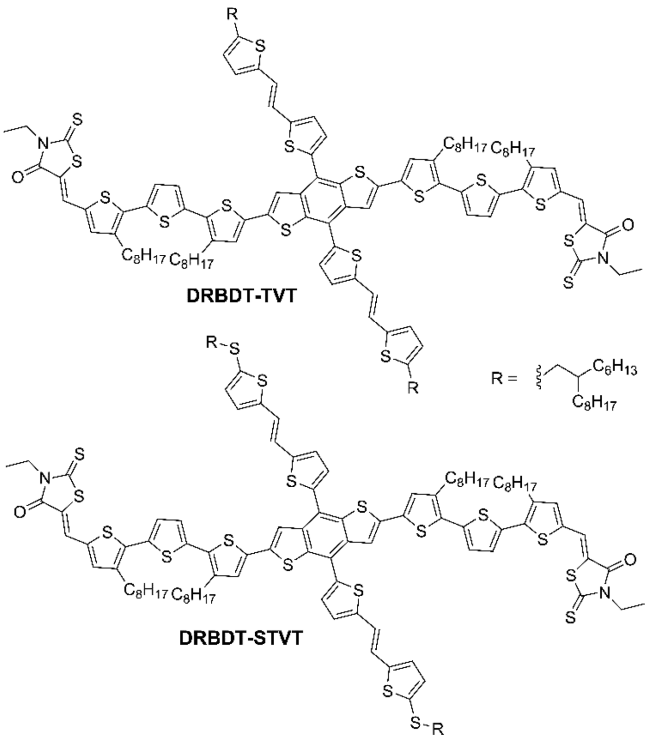

Figure 1. Chemical structures of DRBDT-TVT and DRBDT-STVT.

DRBDT-TVT and DRBDT-STVT were thus designed to have alkyl and alkylthio side chains, respectively. The 3-ethylrhodanine dye was incorporated herein because it has been successfully used as an end group in many donor materials in consideration of its strong absorption and suitable electron-withdrawing property.[64]

In this work, both donors could work well with the fullerene acceptor ($PC_{71}BM$) and nonfullerene acceptor (IDIC), and produce the best PCE value of 6.87% for SM-OSCs and 6.63% for NFASM-OSCs, respectively. To the best of our knowledge, DRBDT-TVT and DRBDT-STVT are among the very few SM donors that can produce over 6.50% PCE in both fullerene and nonfullerene solar cells. Developing these universal SM donors may become a new promising entry point to improve the progress of OSCs.

RESULTS AND DISCUSSION

Material Synthesis and Characterization. DRBDT-TVT and DRBDT-STVT were prepared through Knoevenagel condensation of the dialdehyde intermediates with 3-ethylrhodanine in high yields, and the detailed synthetic procedures including characterization data are presented in the Supporting Information (SI). The two SM donors exhibited good solubility in common solvents, such as chloroform, chlorobenzene (CB), and *o*-dichlorobenzene (*o*-DCB). Thermogravimetric analysis (TGA; Figure S4) shows that both molecules possessed good thermal stability with decomposition temperatures (T_d, 5% weight loss) of 378 and 385 °C, respectively. Density functional theory (DFT) calculations at the B3LYP/6-31G* level were conducted to gain insight into the optimal molecular geometries of DRBDT-TVT and DRBDT-STVT (Figure S1). Side views of both molecules indicate linear backbones with good planarity. The dihedral angle between BDT and TVT side groups was 50.5° for DRBDT-STVT, slightly larger than the 47.6° of DRBDT-TVT.

DOI: 10.1021/acsami.7b17961
ACS Appl. Mater. Interfaces XXXX, XXX, XXX−XXX

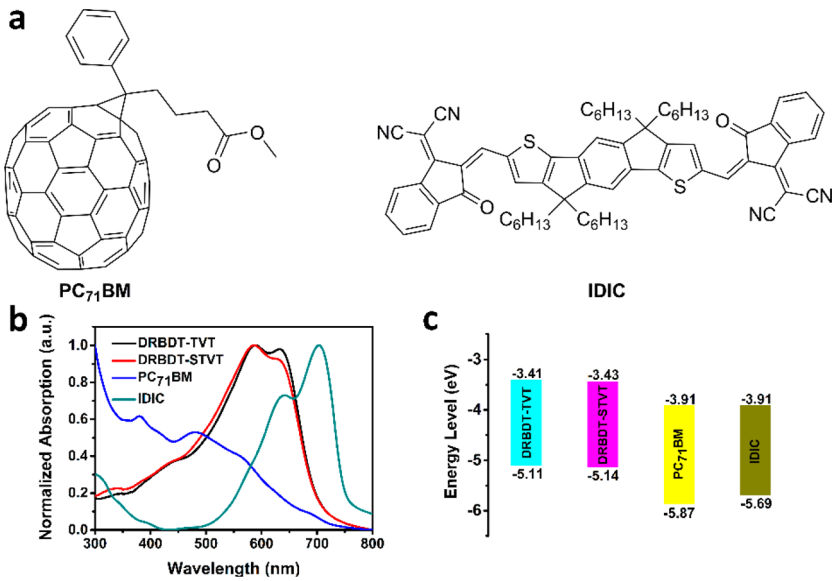

Figure 2. (a) Chemical structures of $PC_{71}BM$ and IDIC. (b) Film absorption spectra of DRBDT-TVT, DRBDT-STVT, $PC_{71}BM$, and IDIC. (c) Energy level diagram of DRBDT-TVT, DRBDT-STVT, $PC_{71}BM$, and IDIC.

Table 1. Optical and Electrochemical Data of DRBDT-TVT and DRBDT-STVT

SM donor	$\lambda_{max,sol}$ (nm)	ε_{sol} (M^{-1} cm^{-1})	$\lambda_{max,film}$ (nm)	ε_{film} (cm^{-1})	E_g^{opt} (eV)	HOMO (eV)	LUMO (eV)	E_g^{cv} (eV)
DRBDT-TVT	412 478	8.0×10^4	587 632	3.3×10^4	1.75	−5.11	−3.41	1.70
DRBDT-STVT	416 462	8.0×10^4	588 630	3.1×10^4	1.76	−5.14	−3.43	1.71

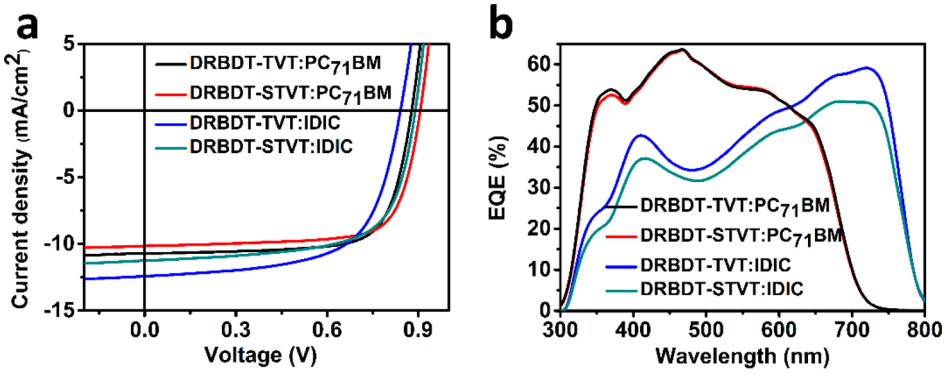

Figure 3. (a) J–V characteristics and (b) EQE spectra of the optimized OSCs with SVA treatment under illumination of AM 1.5 G at 100 mW cm^{-2}.

Optical and Electrochemical Properties. The UV–vis absorption spectra of DRBDT-TVT and DRBDT-STVT in diluted $CHCl_3$ solutions and solid films are illustrated in Figure S2 and Figure 2b, and the relevant data are summarized in Table 1. In solutions, DRBDT-TVT and DRBDT-STVT show broad and strong absorption from 300 to 600 nm and exhibit the maximum absorption peaks (λ_{max}) at 460 and 480 nm, respectively, with a nearly identical maximum absorption coefficient of 8.0×10^4 M^{-1} cm^{-1}. Both molecules display red-shifted and broadened absorption spectra from solutions to films, suggesting strong intermolecular interactions between the conjugated backbones. The film absorption coefficients for DRBDT-TVT and DRBDT-STVT are 3.3×10^4 and 3.1×10^4 cm^{-1}, respectively. Compared with DRBDT-TVT, DRBDT-STVT has slightly blue-shifted absorption in both solution and film, which may be attributed to its larger dihedral angle between STVT side group and BDT unit that hinders molecular packing.[63] The optical bandgaps of DRBDT-TVT and DRBDT-STVT are 1.75 and 1.76 eV, respectively. Cyclic voltammetry (CV) was employed to investigate the electrochemical properties of both molecules in dichloromethane solutions (Figure S3). The HOMO/LUMO levels are estimated to be −5.11/−3.41 eV for DRBDT-TVT, and −5.14/−3.43 eV for DRBDT-STVT (Figure 2c). DRBDT-STVT shows a down-shifted HOMO level attributed to the π-acceptor capability of the sulfur atom, which may lead to higher V_{OC} in the solar cell device.[61,62] The bandgaps of DRBDT-TVT and DRBDT-STVT, calculated from the CV method, are 1.70 and 1.71 eV, respectively, in good agreement to their optical bandgaps.

Photovoltaic Properties. The $PC_{71}BM$ and IDIC were chosen as the representative acceptors to fabricate devices, and their chemical structures are depicted in Figure 2a. It was expected that DRBDT-TVT and DRBDT-STVT should work well with these two acceptors based on the following facts: First, the film absorptions of DRBDT-TVT and DRBDT-STVT are in the range 400–700 nm, which is complementary to the absorption in the ranges 300–500 nm for $PC_{71}BM$ and 500–

DOI: 10.1021/acsami.7b17961
ACS Appl. Mater. Interfaces XXXX, XXX, XXX–XXX

Table 2. Device Parameters of the Optimized SM-OSCs and ASM-OSCs under the Illumination of AM 1.5G, 100 mW cm^{-2}

blend	V_{OC} (V)	J_{SC} (mA cm^{-2})	FF (%)	PCE[a] (%)	J_{SC}^{cal} (mA cm^{-2})
DRBDT-TVT:$PC_{71}BM$[b]	0.879	10.73	72.76	6.87 (6.67 ± 0.20)	10.28
DRBDT-STVT:$PC_{71}BM$[b]	0.907	10.25	73.61	6.84 (6.61 ± 0.23)	10.22
DRBDT-TVT:IDIC[c]	0.840	12.22	64.58	6.63 (6.45 ± 0.18)	11.75
DRBDT-STVT:IDIC[c]	0.887	10.93	67.17	6.51 (6.25 ± 0.25)	10.53

[a]Average data are obtained from 20 devices. [b]With CS_2 SVA treatment for 30 s. [c]With THF SVA treatment for 30 s.

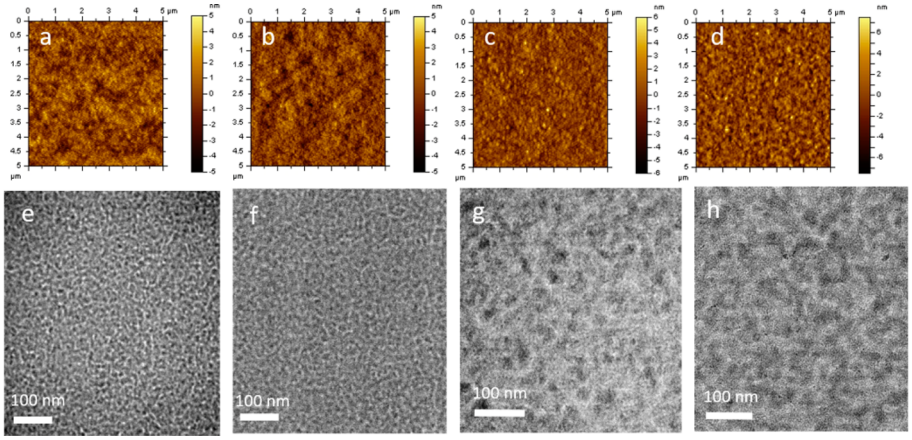

Figure 4. AFM height images of (a) DRBDT-TVT:$PC_{71}BM$ blend film, (b) DRBDT-STVT:$PC_{71}BM$ blend film, (c) DRBDT-TVT:IDIC blend film, and (d) DRBDT-STVT:IDIC blend film with SVA treatment. (e–h) Corresponding TEM images. The scale bars are 100 nm.

800 nm for IDIC. Second, the HOMO/LUMO levels of DRBDT-TVT and DRBDT-STVT are higher than those of $PC_{71}BM$ and IDIC. The proper LUMO offsets provide an effective driving force for charge separation. Third, IDIC exhibits a good electron mobility (μ_e = 1.1 × 10^{-3} cm^2 V^{-1} s^{-1}),[20] which is close to the hole mobility of DRBDT-TVT (μ_h = 8.5 × 10^{-4} cm^2 V^{-1} s^{-1}) and DRBDT-STVT (μ_h = 7.1 × 10^{-4} cm^2 V^{-1} s^{-1}) as measured by the space charge limited current (SCLC) method (Figure S5), ensuring efficient and balanced charge transport in the blend film.

The conventional devices of ITO/PEDOT:PSS/SM donors:$PC_{71}BM$/$PrC_{60}MA$/Al for SM-OSCs and ITO/PEDOT:PSS/SM donors:IDIC/PDIN/Al for NFASM-OSCs were fabricated to evaluate the photovoltaic performance of DRBDT-TVT and DRBDT-STVT. The *J*–*V* curves and external quantum efficiency (EQE) spectra are shown in Figure 3, and the corresponding device parameters are summarized in Table 2. For $PC_{71}BM$ cells, the as-cast devices based on DRBDT-TVT and DRBDT-STVT showed moderate PCEs of 6.27% and 5.86%, respectively, along with relatively low J_{SC}. After solvent vapor annealing (SVA) treatment with CS_2 for 30 s, the PCEs of DRBDT-TVT- and DRBDT-STVT-based devices increased to 6.87% and 6.84%, respectively, with increased J_{SC} and excellent fill factor (FF) over 70%. For IDIC cells, the as-cast devices based on DRBDT-TVT and DRBDT-STVT yielded relatively low PCEs of 3.54% and 3.37%, respectively, with very low J_{SC} and FFs. After SVA treatment with THF for 30 s, the PCEs of DRBDT-TVT- and DRBDT-STVT-based devices rose to 6.63% and 6.51%, respectively, with significantly improved J_{SC} and FFs. Table 1 shows that the V_{OC} values of the as-cast IDIC cells were close to that of the as-cast $PC_{71}BM$ cells for the same donor, consistent with the similar LUMO levels of $PC_{71}BM$ and IDIC. Compared with the optimized $PC_{71}BM$ cells, the optimized IDIC cells gave higher J_{SC} originating from their stronger photoresponse in the near-infrared region. However, the FFs of the optimized IDIC cells were slightly poor, implying that charge recombination was more obvious though most of charge recombination was effectively suppressed in all four types of devices.[65] Compared with the DRBDT-TVT-based devices, the DRBDT-STVT-based devices revealed slightly poor PCEs with lower J_{SC} despite the larger V_{OC} and FFs in both fullerene and nonfullerene solar cells. The higher V_{OC} of the DRBDT-STVT-based devices was attributed to the lowered HOMO level by introduction of sulfur atoms. The lower J_{SC} of DRBDT-STVT-based devices may be due to its slightly poorer absorption and larger lamellar packing distance as discussed blow. The calculated J_{SC} obtained by integration of the EQE curves is listed in Table 2, which is in good agreement with the J_{SC} value measured from the *J*–*V* curves (the error is <5%). During the preparation of this paper, we have been made aware that Li's group has recently fabricated fullerene OSCs consisting of DRBDT-TVT and has obtained the highest PCE up to 5.71%.[66] In comparison, we obtained the highest PCE of 6.87% in fullerene OSCs based on the DRBDT-TVT donor. The significantly higher PCE in this work may be attributed to more ideal film morphology brought by the SVA treatment. Utilization of DRBDT-TVT in all small-molecule nonfullerene solar cells has not yet been reported.

Morphological Characterization. The active layer morphologies were investigated by atomic force microscopy (AFM) and transmission electron microscopy (TEM) (Figure 4). From the AFM images, the SMs/$PC_{71}BM$ and SMs/IDIC blend films present a smooth and uniform surface with root-mean-square (RMS) roughness of 1.15–1.28 nm. From the TEM images, an obvious phase separation can be found after the SVA process, evident by the uniform interpenetration network with well-defined nanofibrils. All the four optimized blends exhibited favorable morphologies for efficient exciton

DOI: 10.1021/acsami.7b17961
ACS Appl. Mater. Interfaces XXXX, XXX, XXX–XXX

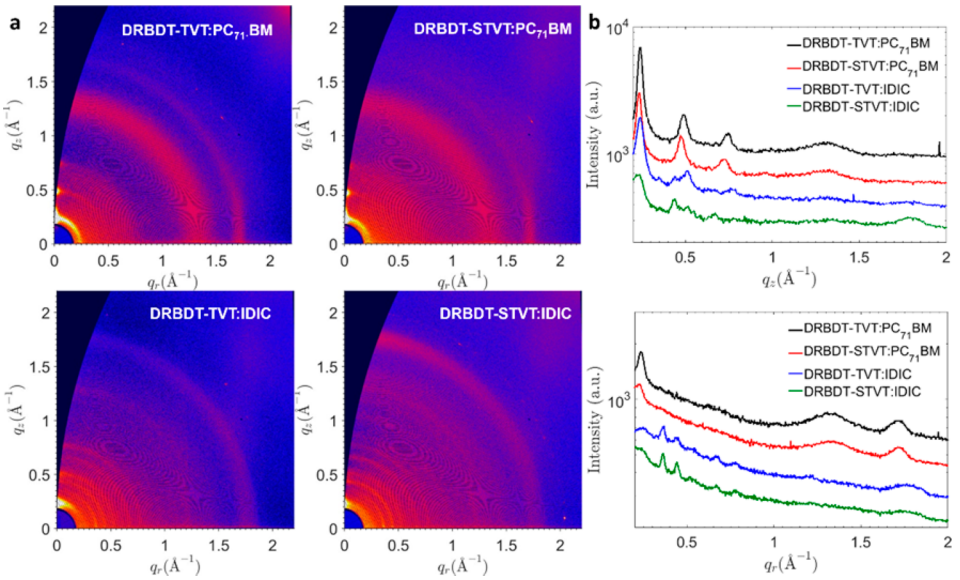

Figure 5. (a) Two-dimensional GIWAXS images of DRBDT-TVT:$PC_{71}BM$, DRBDT-STVT:$PC_{71}BM$, DRBDT-TVT:IDIC, and DRBDT-STVT:IDIC blends with SVA treatment. (b) Corresponding intensity profiles along the out-of-plane (q_z) and in-plane (q_r) directions.

dissociation and charge transport, responsible for the excellent J_{SC} and FFs, resulting in good device performance.

GIWAXS Measurement. Grazing-incidence wide-angle X-ray scattering (GIWAXS) measurements were employed to investigate the crystal structure and orientation of the films (Figure 5).[67,68] The BHJ films blended with $PC_{71}BM$ exhibit similar scattering patterns with up to three orders of the lamellar peaks along the out-of-plane direction and the $\pi-\pi$ peaks along the in-plane direction, suggesting preferential "edge-on" oriented donor domains with stronger crystallinity. It is noted that the ring appearing at $q \sim 1.31$ Å^{-1} originates from the amorphous $PC_{71}BM$ domains. The $\pi-\pi$ stacking distances are similar ($q \approx 1.71$ Å^{-1}, $d \approx 3.67$ Å), indicating similar steric hindrance for both donor molecules. The lamellar stacking distance ($q \approx 0.240$ Å^{-1}, $d \approx 26.2$ Å) of DRBDT-TVT is slightly smaller than that of DRBDT-STVT ($q \approx 0.234$ Å^{-1}, $d \approx 26.9$ Å), most likely because of the relatively shorter alkyl side chain in DRBDT-TVT than the alkylthio side chains in DRBDT-STVT. For the films blended with IDIC, the crystallinity of donor domains decreases significantly, as indicated by the appearance of only the first-order lamellar peaks ($q \approx 0.240$ Å^{-1}, $d \approx 26.2$ Å for DRBDT-TVT and $q \approx 0.234$ Å^{-1}, $d \approx 26.9$ Å for DRBDT-STVT) along the out-of-plane direction, consistent with the relatively lower hole mobility in the films blended with IDIC compared with that of the films blended with $PC_{71}BM$. The lamellar stacking distance of DRBDT-TVT is also smaller than that of DRBDT-STVT, similar to the trend observed in the films blended with $PC_{71}BM$. The rings appearing at $q \approx 0.367$, 0.442, 0.543, 0.671, and 0.784 Å^{-1} are assigned to the scattering of highly crystalline domains of IDIC, commonly observed in fused-ring nonfullerene acceptors.[23,30] Obviously, compared to the pure IDIC film (Figure S10a), the mixing of IDIC with DRBDT-TVT/STVT promotes the crystalline ordering of IDIC domains, which is beneficial to electron transport. The ring appearing at $q \approx 1.78$ Å^{-1} ($d \approx 3.53$ Å) is assigned to the $\pi-\pi$ stacking of IDIC, which is concentrated along the q_z axis for the film of DRBDT-STVT:$PC_{71}BM$, suggesting the existence of weakly "face-on" orientated IDIC crystalline domains to facilitate the efficient electron transport.

Hole and Electron Mobility. The hole mobility (μ_h) and electron mobility (μ_e) of the blend films were tested by the SCLC method (Figure S8, Tables S13 and S14). The hole/electron mobilities for the best DRBDT-TVT/$PC_{71}BM$ and DRBDT-STVT/$PC_{71}BM$ blends were $3.6 \times 10^{-4}/6.7 \times 10^{-4}$ cm^2 V^{-1} s^{-1} ($\mu_h/\mu_e = 0.5$) and $3.4 \times 10^{-4}/6.2 \times 10^{-4}$ cm^2 V^{-1} s^{-1} ($\mu_h/\mu_e = 0.5$), respectively. The hole/electron mobilities for the best DRBDT-TVT/IDIC and DRBDT-STVT/IDIC blends were $1.4 \times 10^{-4}/1.2 \times 10^{-4}$ cm^2 V^{-1} s^{-1} ($\mu_h/\mu_e = 1.1$) and $0.5 \times 10^{-4}/1.0 \times 10^{-4}$ cm^2 V^{-1} s^{-1} ($\mu_h/\mu_e = 0.5$), respectively. Compared with the DRBDT-TVT-based blends, the DRBDT-STVT-based blends showed slightly lower hole and electron mobilities when it was combined with either $PC_{71}BM$ or IDIC, due to their relatively larger lamellar packing distance. In both the fullerene and the nonfullerene devices, the high and balanced hole and electron mobilities enhanced charge transport and suppressed charge recombination, giving rise to high FF.

Charge Recombination. The correlation between J_{SC} and light intensity (P_{light}) was measured to understand the charge recombination in the devices, which was expressed by a power-law formula of $J_{SC} \propto (P_{light})^{\alpha}$ (Figure 6). If the factor α is 1, there is little bimolecular recombination, while $\alpha < 1$ means the existence of charge recombination. The α value of the four optimized devices, DRBDT-TVT/$PC_{71}BM$, DRBDT-STVT/$PC_{71}BM$, DRBDT-TVT/IDIC, and DRBDT-STVT/IDIC was 0.954, 0.948, 0.992, and 0.983, respectively. All the four α values are close to 1, suggesting that the bimolecular recombination was effectively suppressed, and the charge was efficiently collected by the electrodes.

The literature results generally showed that the introduction of sulfur atom into polymers and SMs had a positive effect on the molecular arrangement and photovoltaic performance.[37,46,61,62] However, in this work, the alkylthio-substituted molecule DRBDT-STVT did not produce a much better PCE performance. For the DRBDT-STVT molecule, it is likely that the relatively larger dihedral angle between the STVT side group and the BDT unit decreased the intermolecular interaction, leading to blue-shifted absorption in the solid state. Also the larger lamellar packing distance resulted in lower

DOI: 10.1021/acsami.7b17961
ACS Appl. Mater. Interfaces XXXX, XXX, XXX−XXX

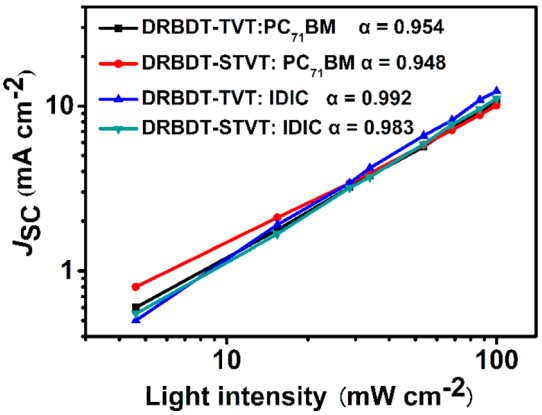

Figure 6. Plots of J_{SC} versus light intensity for SM-OSCs and NFASM-OSCs with SVA treatment.

mobilities for both DRBDT-STVT single component and blend films, compared with that of DRBDT-TVT. Consequently, the DRBDT-STVT-based devices possessed a decreased J_{SC} and slightly lower PCEs. Our results once again demonstrated that it is highly challenging to design SM donors for both fullerene and nonfullerene SM-OSCs, as many factors need to be contemplated and balanced.

CONCLUSION

In summary, two medium-bandgap SM donors, DRBDT-TVT and DRBDT-STVT, were developed, which exhibited complementary absorption, proper energy levels, and optimal blend morphology with $PC_{71}BM$ and IDIC acceptors. The optimized solar cells produced a decent PCE value of 6.87% for SM-OSCs and 6.63% for NFASM-OSCs. These two molecules are rare examples that possess over 6.50% PCEs in both fullerene and nonfullerene solar cells. Our work provides probably the first successful attempt toward developing universal high-performance SM donors with good compatibility with both fullerene acceptors and nonfullerene acceptors, which may accelerate the fundamental research and practical applications of SM-based organic solar cells.

ASSOCIATED CONTENT

Supporting Information

The Supporting Information is available free of charge on the ACS Publications website at DOI: 10.1021/acsami.7b17961.

Details of the materials synthesis; DFT calculations; device fabrication and optimization; and additional characterization data: TGA, AFM, TEM, SCLC, and GIWAXS (PDF)

AUTHOR INFORMATION

Corresponding Authors

*E-mail: yschen99@nankai.edu.cn.
*E-mail: xwzhan@pku.edu.cn.
*E-mail: haoli.zhang@lzu.edu.cn.

ORCID

Xiangfeng Shao: 0000-0002-8710-4122
Yongsheng Chen: 0000-0003-1448-8177
Xiaowei Zhan: 0000-0002-1006-3342
Hao-Li Zhang: 0000-0002-6322-5202

Notes

The authors declare no competing financial interest.

ACKNOWLEDGMENTS

This work is supported by the Ministry of Science and Technology of China (2017YFA0204903), National Natural Science Foundation of China (NSFC. 51733004, 51525303, 2123300, 21522203, 21702085) and 111 Project, Fundamental Research Funds for the Central Universities (lzujbky-2017-11). The authors thank the beamline BL14B1 (Shanghai Synchrotron Radiation Facility) for providing the beam time and help during experiments.

REFERENCES

(1) Cheng, Y.-J.; Yang, S.-H.; Hsu, C.-S. Synthesis of Conjugated Polymers for Organic Solar Cell Applications. *Chem. Rev.* **2009**, *109*, 5868−5923.
(2) Dou, L.; Liu, Y.; Hong, Z.; Li, G.; Yang, Y. Low-Bandgap Near-IR Conjugated Polymers/Molecules for Organic Electronics. *Chem. Rev.* **2015**, *115*, 12633−12665.
(3) Yan, C.; Barlow, S.; Wang, Z.; Yan, H.; Jen, A. K. Y.; Marder, S. R.; Zhan, X. Non-fullerene acceptors for organic solar cells. *Nat. Rev. Mater.* **2018**, *3*, 18003.
(4) Lu, L.; Zheng, T.; Wu, Q.; Schneider, A. M.; Zhao, D.; Yu, L. Recent Advances in Bulk Heterojunction Polymer Solar Cells. *Chem. Rev.* **2015**, *115*, 12666−12731.
(5) Halls, J. J. M.; Walsh, C. A.; Greenham, N. C.; Marseglia, E. A.; Friend, R. H.; Moratti, S. C.; Holmes, A. B. Efficient photodiodes from interpenetrating polymer networks. *Nature* **1995**, *376*, 498−500.
(6) Yu, G.; Gao, J.; Hummelen, J. C.; Wudl, F.; Heeger, A. J. Polymer Photovoltaic Cells - Enhanced Efficiencies Via a Network of Internal Donor-Acceptor Heterojunctions. *Science* **1995**, *270*, 1789−1791.
(7) Li, M.; Gao, K.; Wan, X.; Zhang, Q.; Kan, B.; Xia, R.; Liu, F.; Yang, X.; Feng, H.; Ni, W.; Wang, Y.; Peng, J.; Zhang, H.; Liang, Z.; Yip, H.-L.; Peng, X.; Cao, Y.; Chen, Y. Solution-processed organic tandem solar cells with power conversion efficiencies > 12%. *Nat. Photonics* **2017**, *11*, 85−90.
(8) Ouyang, X.; Peng, R.; Ai, L.; Zhang, X.; Ge, Z. Efficient polymer solar cells employing a non-conjugated small-molecule electrolyte. *Nat. Photonics* **2015**, *9*, 520−524.
(9) He, Z.; Xiao, B.; Liu, F.; Wu, H.; Yang, Y.; Xiao, S.; Wang, C.; Russell, T. P.; Cao, Y. Single-junction polymer solar cells with high efficiency and photovoltage. *Nat. Photonics* **2015**, *9*, 174−179.
(10) Liu, Y.; Zhao, J.; Li, Z.; Mu, C.; Ma, W.; Hu, H.; Jiang, K.; Lin, H.; Ade, H.; Yan, H. Aggregation and morphology control enables multiple cases of high-efficiency polymer solar cells. *Nat. Commun.* **2014**, *5*, 5293.
(11) Zhao, J.; Li, Y.; Yang, G.; Jiang, K.; Lin, H.; Ade, H.; Ma, W.; Yan, H. Efficient organic solar cells processed from hydrocarbon solvents. *Nat. Energy* **2016**, *1*, 15027.
(12) Anctil, A.; Babbitt, C. W.; Raffaelle, R. P.; Landi, B. J. Material and energy intensity of fullerene production. *Environ. Sci. Technol.* **2011**, *45*, 2353−2359.
(13) Lin, Y.; Zhan, X. Non-fullerene acceptors for organic photovoltaics: an emerging horizon. *Mater. Horiz.* **2014**, *1*, 470.
(14) Guo, X.; Facchetti, A.; Marks, T. J. Imide- and amide-functionalized polymer semiconductors. *Chem. Rev.* **2014**, *114*, 8943−9021.
(15) Sun, D.; Meng, D.; Cai, Y.; Fan, B.; Li, Y.; Jiang, W.; Huo, L.; Sun, Y.; Wang, Z. Non-Fullerene-Acceptor-Based Bulk-Heterojunction Organic Solar Cells with Efficiency over 7. *J. Am. Chem. Soc.* **2015**, *137*, 11156−11162.
(16) Dou, C.; Long, X.; Ding, Z.; Xie, Z.; Liu, J.; Wang, L. An Electron-Deficient Building Block Based on the B<−N Unit: An Electron Acceptor for All-Polymer Solar Cells. *Angew. Chem., Int. Ed.* **2016**, *55*, 1436−1440.
(17) Zhong, Y.; Trinh, M. T.; Chen, R.; Wang, W.; Khlyabich, P. P.; Kumar, B.; Xu, Q.; Nam, C. Y.; Sfeir, M. Y.; Black, C.; Steigerwald, M. L.; Loo, Y. L.; Xiao, S.; Ng, F.; Zhu, X. Y.; Nuckolls, C. Efficient

organic solar cells with helical perylene diimide electron acceptors. *J. Am. Chem. Soc.* **2014**, *136*, 15215−15221.
(18) Kim, T.; Kim, J. H.; Kang, T. E.; Lee, C.; Kang, H.; Shin, M.; Wang, C.; Ma, B.; Jeong, U.; Kim, T. S.; Kim, B. J. Flexible, highly efficient all-polymer solar cells. *Nat. Commun.* **2015**, *6*, 8547.
(19) Lin, Y.; Wang, J.; Zhang, Z. G.; Bai, H.; Li, Y.; Zhu, D.; Zhan, X. An electron acceptor challenging fullerenes for efficient polymer solar cells. *Adv. Mater.* **2015**, *27*, 1170−1174.
(20) Lin, Y.; He, Q.; Zhao, F.; Huo, L.; Mai, J.; Lu, X.; Su, C. J.; Li, T.; Wang, J.; Zhu, J.; Sun, Y.; Wang, C.; Zhan, X. A Facile Planar Fused-Ring Electron Acceptor for As-Cast Polymer Solar Cells with 8.71% Efficiency. *J. Am. Chem. Soc.* **2016**, *138*, 2973−2976.
(21) Wang, J.; Wang, W.; Wang, X.; Wu, Y.; Zhang, Q.; Yan, C.; Ma, W.; You, W.; Zhan, X. Enhancing Performance of Nonfullerene Acceptors via Side-Chain Conjugation Strategy. *Adv. Mater.* **2017**, *29*, 1702125.
(22) Zhao, F.; Dai, S.; Wu, Y.; Zhang, Q.; Wang, J.; Jiang, L.; Ling, Q.; Wei, Z.; Ma, W.; You, W.; Wang, C.; Zhan, X. Single-Junction Binary-Blend Nonfullerene Polymer Solar Cells with 12.1% Efficiency. *Adv. Mater.* **2017**, *29*, 1700144.
(23) Wang, W.; Yan, C.; Lau, T. K.; Wang, J.; Liu, K.; Fan, Y.; Lu, X.; Zhan, X. Fused Hexacyclic Nonfullerene Acceptor with Strong Near-Infrared Absorption for Semitransparent Organic Solar Cells with 9.77% Efficiency. *Adv. Mater.* **2017**, *29*, 1701308.
(24) Yao, H.; Cui, Y.; Yu, R.; Gao, B.; Zhang, H.; Hou, J. Design, Synthesis, and Photovoltaic Characterization of a Small Molecular Acceptor with an Ultra-Narrow Band Gap. *Angew. Chem., Int. Ed.* **2017**, *56*, 3045−3049.
(25) Qiu, N.; Zhang, H.; Wan, X.; Li, C.; Ke, X.; Feng, H.; Kan, B.; Zhang, H.; Zhang, Q.; Lu, Y.; Chen, Y. A New Nonfullerene Electron Acceptor with a Ladder Type Backbone for High-Performance Organic Solar Cells. *Adv. Mater.* **2017**, *29*, 1604964.
(26) Li, S.; Ye, L.; Zhao, W.; Zhang, S.; Mukherjee, S.; Ade, H.; Hou, J. Energy-Level Modulation of Small-Molecule Electron Acceptors to Achieve over 12% Efficiency in Polymer Solar Cells. *Adv. Mater.* **2016**, *28*, 9423−9429.
(27) Lin, Y.; Zhao, F.; He, Q.; Huo, L.; Wu, Y.; Parker, T. C.; Ma, W.; Sun, Y.; Wang, C.; Zhu, D.; Heeger, A. J.; Marder, S. R.; Zhan, X. High-Performance Electron Acceptor with Thienyl Side Chains for Organic Photovoltaics. *J. Am. Chem. Soc.* **2016**, *138*, 4955−4961.
(28) Bin, H.; Gao, L.; Zhang, Z. G.; Yang, Y.; Zhang, Y.; Zhang, C.; Chen, S.; Xue, L.; Yang, C.; Xiao, M.; Li, Y. 11.4% Efficiency non-fullerene polymer solar cells with trialkylsilyl substituted 2D-conjugated polymer as donor. *Nat. Commun.* **2016**, *7*, 13651.
(29) Bin, H.; Zhang, Z. G.; Gao, L.; Chen, S.; Zhong, L.; Xue, L.; Yang, C.; Li, Y. Non-Fullerene Polymer Solar Cells Based on Alkylthio and Fluorine Substituted 2D-Conjugated Polymers Reach 9.5% Efficiency. *J. Am. Chem. Soc.* **2016**, *138*, 4657−4664.
(30) Yang, Y.; Zhang, Z. G.; Bin, H.; Chen, S.; Gao, L.; Xue, L.; Yang, C.; Li, Y. Side-Chain Isomerization on an n-type Organic Semiconductor ITIC Acceptor Makes 11.77% High Efficiency Polymer Solar Cells. *J. Am. Chem. Soc.* **2016**, *138*, 15011−15018.
(31) Shi, X.; Zuo, L.; Jo, S. B.; Gao, K.; Lin, F.; Liu, F.; Jen, A. K. Y. Design of a highly crystalline low band-gap fused-ring electron acceptor for high efficiency solar cells with low energy loss. *Chem. Mater.* **2017**, *29*, 8369−8376.
(32) Cui, Y.; Yao, H.; Gao, B.; Qin, Y.; Zhang, S.; Yang, B.; He, C.; Xu, B.; Hou, J. Fine-Tuned Photoactive and Interconnection Layers for Achieving over 13% Efficiency in a Fullerene-Free Tandem Organic Solar Cell. *J. Am. Chem. Soc.* **2017**, *139*, 7302−7309.
(33) Zhao, W.; Li, S.; Yao, H.; Zhang, S.; Zhang, Y.; Yang, B.; Hou, J. Molecular Optimization Enables over 13% Efficiency in Organic Solar Cells. *J. Am. Chem. Soc.* **2017**, *139* (21), 7148−7151.
(34) Mei, J.; Bao, Z. Side Chain Engineering in Solution-Processable Conjugated Polymers. *Chem. Mater.* **2014**, *26*, 604−615.
(35) Dennler, G.; Scharber, M. C.; Brabec, C. J. Polymer-Fullerene Bulk-Heterojunction Solar Cells. *Adv. Mater.* **2009**, *21*, 1323−1338.
(36) Liu, Y.; Chen, C. C.; Hong, Z.; Gao, J.; Yang, Y. M.; Zhou, H.; Dou, L.; Li, G.; Yang, Y. Solution-processed small-molecule solar cells: breaking the 10% power conversion efficiency. *Sci. Rep.* **2013**, *3*, 3356.
(37) Kan, B.; Zhang, Q.; Li, M.; Wan, X.; Ni, W.; Long, G.; Wang, Y.; Yang, X.; Feng, H.; Chen, Y. Solution-processed organic solar cells based on dialkylthiol-substituted benzodithiophene unit with efficiency near 10%. *J. Am. Chem. Soc.* **2014**, *136*, 15529−15532.
(38) Kan, B.; Li, M.; Zhang, Q.; Liu, F.; Wan, X.; Wang, Y.; Ni, W.; Long, G.; Yang, X.; Feng, H.; Zuo, Y.; Zhang, M.; Huang, F.; Cao, Y.; Russell, T. P.; Chen, Y. A series of simple oligomer-like small molecules based on oligothiophenes for solution-processed solar cells with high efficiency. *J. Am. Chem. Soc.* **2015**, *137*, 3886−3893.
(39) Zhou, J.; Zuo, Y.; Wan, X.; Long, G.; Zhang, Q.; Ni, W.; Liu, Y.; Li, Z.; He, G.; Li, C.; Kan, B.; Li, M.; Chen, Y. Solution-processed and high-performance organic solar cells using small molecules with a benzodithiophene unit. *J. Am. Chem. Soc.* **2013**, *135*, 8484−8487.
(40) Zhou, J.; Wan, X.; Liu, Y.; Zuo, Y.; Li, Z.; He, G.; Long, G.; Ni, W.; Li, C.; Su, X.; Chen, Y. Small molecules based on benzo[1,2-b:4,5-b']dithiophene unit for high-performance solution-processed organic solar cells. *J. Am. Chem. Soc.* **2012**, *134*, 16345−16351.
(41) Collins, S. D.; Ran, N. A.; Heiber, M. C.; Nguyen, T.-Q. Small is Powerful: Recent Progress in Solution-Processed Small Molecule Solar Cells. *Adv. Energy Mater.* **2017**, *7*, 1602242.
(42) Gao, K.; Li, L.; Lai, T.; Xiao, L.; Huang, Y.; Huang, F.; Peng, J.; Cao, Y.; Liu, F.; Russell, T. P.; Janssen, R. A. J.; Peng, X. Deep Absorbing Porphyrin Small Molecule for High-Performance Organic Solar Cells with Very Low Energy Losses. *J. Am. Chem. Soc.* **2015**, *137*, 7282−7285.
(43) Coughlin, J. E.; Henson, Z. B.; Welch, G. C.; Bazan, G. C. Design and Synthesis of Molecular Donors for Solution-Processed High-Efficiency Organic Solar Cells. *Acc. Chem. Res.* **2014**, *47*, 257−270.
(44) Roncali, J.; Leriche, P.; Blanchard, P. Molecular materials for organic photovoltaics: small is beautiful. *Adv. Mater.* **2014**, *26*, 3821−3838.
(45) Mishra, A.; Bauerle, P. Small molecule organic semiconductors on the move: promises for future solar energy technology. *Angew. Chem., Int. Ed.* **2012**, *51*, 2020−2067.
(46) Wan, J.; Xu, X.; Zhang, G.; Li, Y.; Feng, K.; Peng, Q. Highly efficient halogen-free solvent processed small-molecule organic solar cells enabled by material design and device engineering. *Energy Environ. Sci.* **2017**, *10*, 1739−1745.
(47) Deng, D.; Zhang, Y.; Zhang, J.; Wang, Z.; Zhu, L.; Fang, J.; Xia, B.; Wang, Z.; Lu, K.; Ma, W.; Wei, Z. Fluorination-enabled optimal morphology leads to over 11% efficiency for inverted small-molecule organic solar cells. *Nat. Commun.* **2016**, *7*, 13740.
(48) Yang, L.; Zhang, S.; He, C.; Zhang, J.; Yao, H.; Yang, Y.; Zhang, Y.; Zhao, W.; Hou, J. New Wide Band Gap Donor for Efficient Fullerene-Free All-Small-Molecule Organic Solar Cells. *J. Am. Chem. Soc.* **2017**, *139*, 1958−1966.
(49) Bin, H.; Yang, Y.; Zhang, Z. G.; Ye, L.; Ghasemi, M.; Chen, S.; Zhang, Y.; Zhang, C.; Sun, C.; Xue, L.; Yang, C.; Ade, H.; Li, Y. 9.73% Efficiency Nonfullerene All Organic Small Molecule Solar Cells with Absorption-Complementary Donor and Acceptor. *J. Am. Chem. Soc.* **2017**, *139*, 5085−5094.
(50) Qiu, B.; Xue, L.; Yang, Y.; Bin, H.; Zhang, Y.; Zhang, C.; Xiao, M.; Park, K.; Morrison, W.; Zhang, Z.-G.; Li, Y. All-Small-Molecule Nonfullerene Organic Solar Cells with High Fill Factor and High Efficiency over 10%. *Chem. Mater.* **2017**, *29*, 7543−7553.
(51) Kwon, O. K.; Park, J. H.; Kim, D. W.; Park, S. K.; Park, S. Y. An all-small-molecule organic solar cell with high efficiency nonfullerene acceptor. *Adv. Mater.* **2015**, *27*, 1951−1956.
(52) Douglas, J. D.; Chen, M. S.; Niskala, J. R.; Lee, O. P.; Yiu, A. T.; Young, E. P.; Frechet, J. M. Solution-processed, molecular photovoltaics that exploit hole transfer from non-fullerene, n-type materials. *Adv. Mater.* **2014**, *26*, 4313−4319.
(53) Huang, J.; Wang, X.; Zhang, X.; Niu, Z.; Lu, Z.; Jiang, B.; Sun, Y.; Zhan, C.; Yao, J. Additive-assisted control over phase-separated nanostructures by manipulating alkylthienyl position at donor

DOI: 10.1021/acsami.7b17961
ACS Appl. Mater. Interfaces XXXX, XXX, XXX−XXX

backbone for solution-processed, non-fullerene, all-small-molecule solar cells. *ACS Appl. Mater. Interfaces* **2014**, *6*, 3853−3862.
(54) Sharenko, A.; Proctor, C. M.; van der Poll, T. S.; Henson, Z. B.; Nguyen, T. Q.; Bazan, G. C. A high-performing solution-processed small molecule:perylene diimide bulk heterojunction solar cell. *Adv. Mater.* **2013**, *25*, 4403−4406.
(55) Liang, N.; Meng, D.; Ma, Z.; Kan, B.; Meng, X.; Zheng, Z.; Jiang, W.; Li, Y.; Wan, X.; Hou, J.; Ma, W.; Chen, Y.; Wang, Z. Triperylene Hexaimides Based All-Small-Molecule Solar Cells with an Efficiency over 6% and Open Circuit Voltage of 1.04 V. *Adv. Energy Mater.* **2017**, *7*, 1601664.
(56) Lin, Y.; Wang, J.; Li, T.; Wu, Y.; Wang, C.; Han, L.; Yao, Y.; Ma, W.; Zhan, X. Efficient fullerene-free organic solar cells based on fused-ring oligomer molecules. *J. Mater. Chem. A* **2016**, *4*, 1486−1494.
(57) An, M.; Xie, F.; Geng, X.; Zhang, J.; Jiang, J.; Lei, Z.; He, D.; Xiao, Z.; Ding, L. A High-Performance D-A Copolymer Based on Dithieno[3,2-b:2′,3′-d]Pyridin-5(4H)-One Unit Compatible with Fullerene and Nonfullerene Acceptors in Solar Cells. *Adv. Energy Mater.* **2017**, *7*, 1602509.
(58) Yao, H.; Ye, L.; Zhang, H.; Li, S.; Zhang, S.; Hou, J. Molecular Design of Benzodithiophene-Based Organic Photovoltaic Materials. *Chem. Rev.* **2016**, *116*, 7397−7457.
(59) Yao, H.; Zhang, H.; Ye, L.; Zhao, W.; Zhang, S.; Hou, J. Molecular Design and Application of a Photovoltaic Polymer with Improved Optical Properties and Molecular Energy Levels. *Macromolecules* **2015**, *48*, 3493−3499.
(60) Chung, H.-S.; Lee, W.-H.; Song, C. E.; Shin, Y.; Kim, J.; Lee, S. K.; Shin, W. S.; Moon, S.-J.; Kang, I.-N. Highly Conjugated Side-Chain-Substituted Benzo[1,2-b:4,5-b′]dithiophene-Based Conjugated Polymers for Use in Polymer Solar Cells. *Macromolecules* **2014**, *47*, 97−105.
(61) Cui, C.; He, Z.; Wu, Y.; Cheng, X.; Wu, H.; Li, Y.; Cao, Y.; Wong, W.-Y. High-performance polymer solar cells based on a 2D-conjugated polymer with an alkylthio side-chain. *Energy Environ. Sci.* **2016**, *9*, 885−891.
(62) Cui, C.; Wong, W.-Y.; Li, Y. Improvement of open-circuit voltage and photovoltaic properties of 2D-conjugated polymers by alkylthio substitution. *Energy Environ. Sci.* **2014**, *7*, 2276−2284.
(63) Kan, B.; Zhang, Q.; Liu, F.; Wan, X.; Wang, Y.; Ni, W.; Yang, X.; Zhang, M.; Zhang, H.; Russell, T. P.; Chen, Y. Small Molecules Based on Alkyl/Alkylthio-thieno[3,2-b]thiophene-Substituted Benzo[1,2-b:4,5-b′]dithiophene for Solution-Processed Solar Cells with High Performance. *Chem. Mater.* **2015**, *27*, 8414−8423.
(64) Zhou, J.; Wan, X.; Liu, Y.; Long, G.; Wang, F.; Li, Z.; Zuo, Y.; Li, C.; Chen, Y. A Planar Small Molecule with Dithienosilole Core for High Efficiency Solution-Processed Organic Photovoltaic Cells. *Chem. Mater.* **2011**, *23*, 4666−4668.
(65) Guo, X.; Zhou, N.; Lou, S. J.; Smith, J.; Tice, D. B.; Hennek, J. W.; Ortiz, R. P.; Navarrete, J. T. L.; Li, S.; Strzalka, J.; Chen, L. X.; Chang, R. P. H.; Facchetti, A.; Marks, T. J. Polymer solar cells with enhanced fill factors. *Nat. Photonics* **2013**, *7*, 825−833.
(66) Zhu, K.; Tang, D.; Zhang, K.; Wang, Z.; Ding, L.; Liu, Y.; Yuan, L.; Fan, J.; Song, B.; Zhou, Y.; Li, Y. A two-dimension-conjugated small molecule for efficient ternary organic solar cells. *Org. Electron.* **2017**, *48*, 179−187.
(67) Mai, J.; Lu, H.; Lau, T.-K.; Peng, S.-H.; Hsu, C.-S.; Hua, W.; Zhao, N.; Xiao, X.; Lu, X. High efficiency ternary organic solar cell with morphology-compatible polymers. *J. Mater. Chem. A* **2017**, *5*, 11739−11745.
(68) Mai, J.; Lau, T.-K.; Li, J.; Peng, S.-H.; Hsu, C.-S.; Jeng, U. S.; Zeng, J.; Zhao, N.; Xiao, X.; Lu, X. Understanding Morphology Compatibility for High-Performance Ternary Organic Solar Cells. *Chem. Mater.* **2016**, *28*, 6186−6195.

DOI: 10.1021/acsami.7b17961
ACS Appl. Mater. Interfaces XXXX, XXX, XXX−XXX